Inhibitory effect and mechanism of hirsuteine on NCI-H1299 lung cancer cell lines

XUELIN YUN[1], HAILONG QIN[1], BIN DU[2], YU PENG[1], YULING LIU[1] and BIXIAN YANG[2]

[1]College of Pharmacy, Guizhou University of Traditional Chinese Medicine, Guiyang, Guizhou 550025;
[2]College of Food and Pharmacy Engineering, Guiyang University, Guiyang, Guizhou 550005, P.R. China

Abstract. Traditionally, the bark of *Uncaria rhynchophylla* (UR) has been employed for the treatment of hypertension, cancer, convulsions, haemorrhage, autoimmune disorders and other ailments. The primary aim of the present study was to explore the antiproliferative activity of hirsuteine (HTE) isolated from UR over a range of concentrations in human NSCLC NCI-H1299 cells and to explore the mechanisms underlying its therapeutic efficacy. The effects of HTE on cell viability were examined using Cell Counting Kit-8 (CCK-8) and colony formation assays, while apoptosis was assessed by flow cytometry. Cell cycle progression was additionally evaluated via propidium iodide staining, while reverse transcription-quantitative PCR and western blotting methods were employed to assess the protein levels and genes related to apoptosis and progression of the cell cycle, respectively. NCI-H1299 cell proliferation was markedly suppressed by HTE in a time- and dose-dependent manner. However, clear changes in cell morphology were also induced, resulting in G0-G1 phase cell cycle arrest, which was associated with cyclin E and CDK2 downregulation. HTE additionally induced robust NSCLC NCI-H1299 cell apoptosis, downregulation of Bcl-2 and upregulation of cytoplasmic cytochrome C, Bax, Apaf1, cleaved caspase-3 and cleaved caspase-9, which together drove the observed apoptotic cell death. HTE could effectively suppress human NSCLC NCI-H1299 cell growth by inducing apoptotic death in a dose-dependent fashion *in vitro*, therefore elucidating the mechanism by which this phytomedicine acts as a potent anticancer compound that warrants study as a treatment for human NSCLC patients.

Correspondence to: Professor Bixian Yang, College of Food and Pharmacy Engineering, Guiyang University, 103 Jianlongdong Road, Guiyang, Guizhou 550005, P.R. China
E-mail: bixiany@163.com

Introduction

Lung cancers are some of the most common and deadly cancers worldwide, with a poor prognosis for those who are diagnosed (1). Non-small cell lung cancer (NSCLC) accounts for 85% of all lung cancer cases (2), with patients exhibiting low 5-year survival rates (2-4). While a range of treatments, including surgery, chemotherapy, radiotherapy and immunotherapy, have improved NSCLC patient survival outcomes, tumor recurrence and metastasis remain common and are associated with poor prognosis (5-7). Although targeted treatment and immunotherapy-based interventions have made some progress in the treatment of metastatic NSCLC, these treatments are extremely expensive, such that they are not widely accessible to the majority of affected patients (8,9). The use of immune checkpoint inhibitors (ICIs) is an attractive treatment option for both patients and clinicians. First, these compounds have a wide range of activities (10). Second, they often induce durable disease control. For example, nivolumab is currently associated with a total 5-year survival rate of 34% in patients with advanced melanoma, while its effects against other cancers are similar. Third, ICIs usually have good toxicity characteristics (particularly anti-PD1/PD-L1 monotherapy) (11). Although ICIs have achieved great success in clinical practice and become a milestone in anticancer treatment, there are still certain clinical challenges with ICI treatments, including resistance mechanisms, individual-level efficacy differences, immune-related adverse reactions and highly progressive diseases (12-14). Determining reliable predictive biomarkers of efficacy, particularly toxicity, has been a major challenge.

The clinical efficacy of CDK4/6 inhibitors in NSCLC depends on the development of predictive biomarkers and biologically rational combination therapy, which may include the addition of growth factor pathway inhibitors in patients with signal transduction pathway mutations or the addition of ICIs in patients with immunostimulatory tumor phenotypes. Based on these, more basic and clinical studies are needed explore the precise beneficiaries of CDK4/6 inhibitors in NSCLC treatment in the future (15). It is thus vital that novel low-cost treatments for advanced NSCLC be developed that can reliably treat this cancer type.

Traditional Chinese medicine (TCM) has long been practiced in China to treat human diseases for thousands of years.

It is a valuable source for drug discovery campaigns (16). The traditional Chinese medicine *Uncaria* has a long history, and *Uncaria rhynchophylla* (UR; Gou-Teng in Chinese), a member of the *Uncaria* genus of the *Rubiaceae* family, is found primarily in southern China. In the practice of traditional Chinese medicine, UR was recorded in the famous TCM monograph Ming Yi Bie Lu and has long been used in China and Japan to extinguish wind, pacify the liver, clear heat and arrest convulsions (17). It is often clinically used in the treatment of central nervous system and cardiovascular diseases, including hypertension, epilepsy, dizziness, convulsions, preeclampsia and tremor (17). To date, a variety of compounds have been isolated from this medicine, including alkaloids, quinolates, terpenes and steroids, particularly indole and oxindole alkaloids, i.e., isorhynchophylline, rhynchophylline, corynoxeine, isocorynoxeine, hirsutine (HTI), hirsuteine (HTE) (PubChem ID, 169699) (Fig. 1) and geissoschizine methyl ether (18,19). These alkaloids possess a variety of pharmacological actions, together with a neuroprotective effect (20-22), a vasodilatation effect (23-25), a 5-HT3 receptor binding effect (26) and anticonvulsant effects (27). HTI and HTE were two alkaloid monomers extracted from the traditional Chinese medicine UR, which have pharmacological effects including antihypertension, anti-infection and heart protection. In terms of chemical structure, HTE has one more double bond and two less hydrogen atoms than HTI (PubChem ID, 3037884), resulting in the change of the chemical properties between the two substances. In terms of chemical structure, that is why the antiproliferative activity of HTE is not as strong as that of HTI (28). These findings indicated that *Uncaria* hook alkaloids are the most important constituents when studying HTE efficacy.

Previous studies have demonstrated that HTE could suppress HepG2 human tumor cell migration and proliferation in a dose-dependent manner, protecting against glutamate-induced cell death in PC12 cells or cultured cerebellar granule cells (29-31). A recent study by the authors showed that HTE could enhance the inhibition of T-cell leukemia Jurkat Clone E6-1 cell proliferation (32). However, no studies to date have assessed the ability of HTE to suppress NSCLC NCI-H1299 cell growth, nor have the underlying pathways governing the pro-apoptotic and antitumor activity of this alkaloid drug been explored in detail.

In the present study, the antiproliferative effect of HTE and its mechanism of action in human NSCLC NCI-H1299 cells were explored, revealing the ability of this alkaloid agent to cause apoptosis and cell cycle arrest in these malignant cells.

Materials and methods

Reagents. HTE (ST17300105, 5 mg/dose, ≥98% pure) was obtained from Shanghai Standard Technology Co., Ltd.

Cell lines and cell culture. Human NCI-H1299 cells were acquired from the Institute of Biochemistry (Shanghai, China) and were cultured in RPMI-1640 (Invitrogen; Thermo Fisher Scientific, Inc.) culture medium at 37°C with 5% CO_2 following incubation under a humidified atmosphere. Human THLE-2 hepatocytes and normal BEAS-2B cells were obtained from Nanjing KeyGen Biotech Co., Ltd. and subsequently cultured
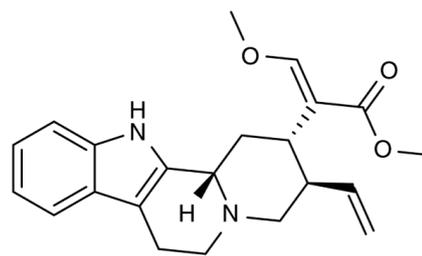
Figure 1. Chemical structure of hirsuteine (MW=366.45 Da).

in Dulbecco's modified Eagle's medium (HyClone; Cytiva). Media were supplemented with pen/strep and 10% FBS (Gibco; Thermo Fisher Scientific, Inc.).

Drug treatments. HTE was suspended in DMSO and stored at -20°C at a stock concentration of 100 mM. RPMI-1640 medium was used to dilute the stock to 0, 10, 20 and 40 μM. The final DMSO concentration in each working solution was kept at 0.1%. In the untreated cell group, RPMI-1640 with 0.1% DMSO was used.

Cell counting kit-8 (CCK-8) assay. Cell proliferation was measured using a CCK-8 assay. Briefly, NCI-H1299 cells at a density of 10,000 cells per well were added to 96-well plates in complete F12K media, with samples being prepared in triplicate. Next, the cells were exposed to a range of HTE concentrations for 24, 48 and 72 h, after which 100 μl CCK-8 solution (Beyotime Institute of Biotechnology) was mixed with the cells for another 4 h of incubation at 37°C. Then, an assay using water-soluble tetrazolium salt was performed to assess cell proliferation by quantifying the absorbance at 450 nm with the help of a microplate reader (Bio-Rad Laboratories, Inc.) according to the manufacturer's protocol. The assay protocols for THLE-2 and BEAS-2B cells were as aforementioned, with cells plated at 4,000 cells/well and treated for 48 h with a range of HTE concentrations prior to CCK-8 reagent addition.

Colony formation assay. To assess cell proliferation, 2-5x10³ cells were added in triplicate to six-well plates. After 24 h, cells were treated with different HTE concentrations (0, 10, 20 and 40 μM). After being cultured for 14 days, the cells were washed twice with PBS, fixed for 15 min with 75% ethanol and stained for 20 min at room temperature with 0.1% crystal violet (Beyotime Institute of Biotechnology), with all colonies containing ≥30 cells being counted manually. Plate images were captured using an Epson scanner (Seiko Epson Corporation).

Apoptosis staining. Flow cytometry was carried out to detect cell apoptosis after labelling with Annexin V-FITC. After harvesting using 0.25% trypsin and spinning down for 3 min at 300 x g NCI-H1299 cells in the logarithmic phase of growth were seeded for 24 h in six-well plates at a density of 3x10⁵ cells/well. A range of HTE concentrations (0, 10, 20 and 40 μM) was applied to the cells for 48 h with 0.1% DMSO as the negative control. After three washes with chilled PBS, the cells were collected and resuspended in 500 μl of cold binding buffer. Incubation was performed for 15 min at room
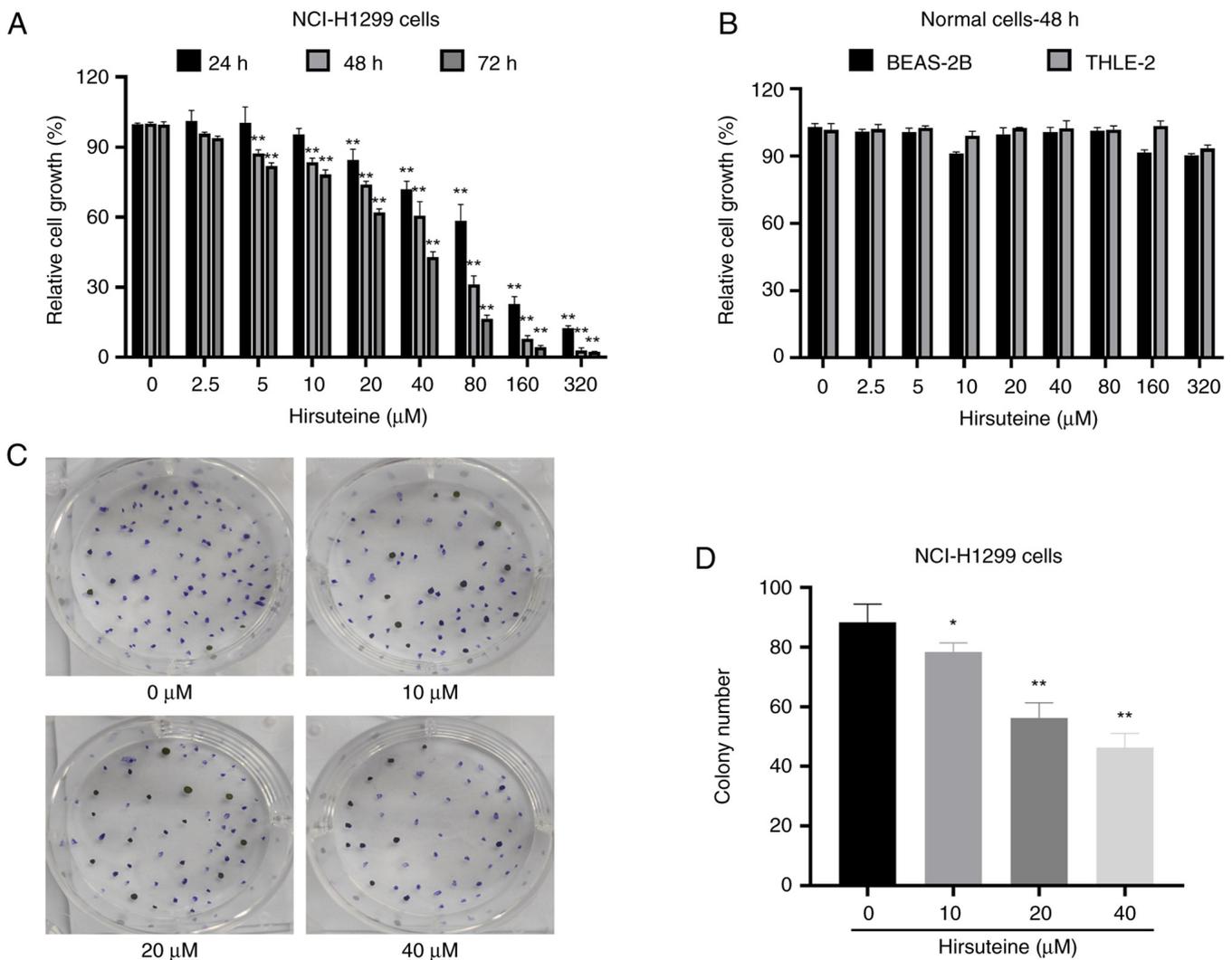
Figure 2. HTE inhibits NCI-H1299 cell proliferation and colony formation. (A) NCI-H1299 cells were treated with HTE. After incubation for 24, 48 or 72 h, the proliferation rates were measured by CCK-8 assay. (B) BEAS-2B and THLE-2 cells were treated with HTE. After incubation for 48 h, the proliferation rates were measured by CCK-8 assay. (C) Cell colonies were stained with crystal violet and observed under an inverted microscope. (D) Statistical analysis of the colony formation of NCI-H1299 cells treated with HTE. All data are expressed as the mean ± SD of three independent experiments. $^*P<0.05$ and $^{**}P<0.01$ compared with the control. HTE, hirsuteine; CCK-8, Cell Counting Kit-8.

temperature in the dark following mixing with 5 μl of Annexin V-FITC and 5 μl of propidium iodide (PI). A CytoFLEX flow cytometry instrument (Beckman Coulter, Inc.) was used to analyze the samples, and the data were processed using FlowJo V10.0 software (Becton, Dickinson and Company). All experimental data were acquired in triplicate.

Cell cycle analysis. Flow cytometry was performed to analyze the cell cycle. Briefly, cells in the log phase were plated at a density of 3x10^5 cells/well in a six-well plate and incubated for 24 h. After incubation, the medium was exchanged for complete medium containing a range of HTE concentrations (0, 10, 20 and 40 μM) for an additional 48 h. Cells were then harvested with 0.25% trypsin, centrifuged at 4˚C for 3 min at 300 x g washed once with PBS, and fixed overnight at 4˚C with 70% chilled ethanol. After overnight incubation, the cells were spun down again, treated with 100 μl of RNase A (50 μg/ml), and resuspended in a water bath at 37˚C for 30 min. The cells were then stained for 30 min at 4˚C in the dark with 400 μl

of PI (50 μg/ml). All samples were evaluated by using the FACScan system (BD Biosciences). Data were examined by Cell-Quest software (BD Biosciences). All experiments were performed three times independently.

Western blotting. Following 48 h of treatment with HTE (0, 10, 20 and 40 μM), chilled RIPA buffer (Beyotime Institute of Biotechnology) was used for cell lysis for 30 min, after which the cell lysates were centrifuged at 4˚C for 15 min at 13,201 x g. The amounts of protein in the supernatants were estimated by BCA assay (Beyotime Institute of Biotechnology). Next, separation of equal amounts of protein (40 μg) was achieved using 10-12% SDS-PAGE. After separation, the proteins were transferred to PVDF membranes. Membranes were blocked in 5% non-fat milk in TBS containing 0.1% Tween-20 (TBST) for 2 h at room temperature. Overnight incubation was then performed at 4˚C with primary anti-CDK2 (cat. no. A0294; ABclonal Biotech Co., Ltd.), anti-cyclin E (cat. no. A14225; ABclonal Biotech Co., Ltd.), anti-Bax (cat. no. 50599-2-Ig;
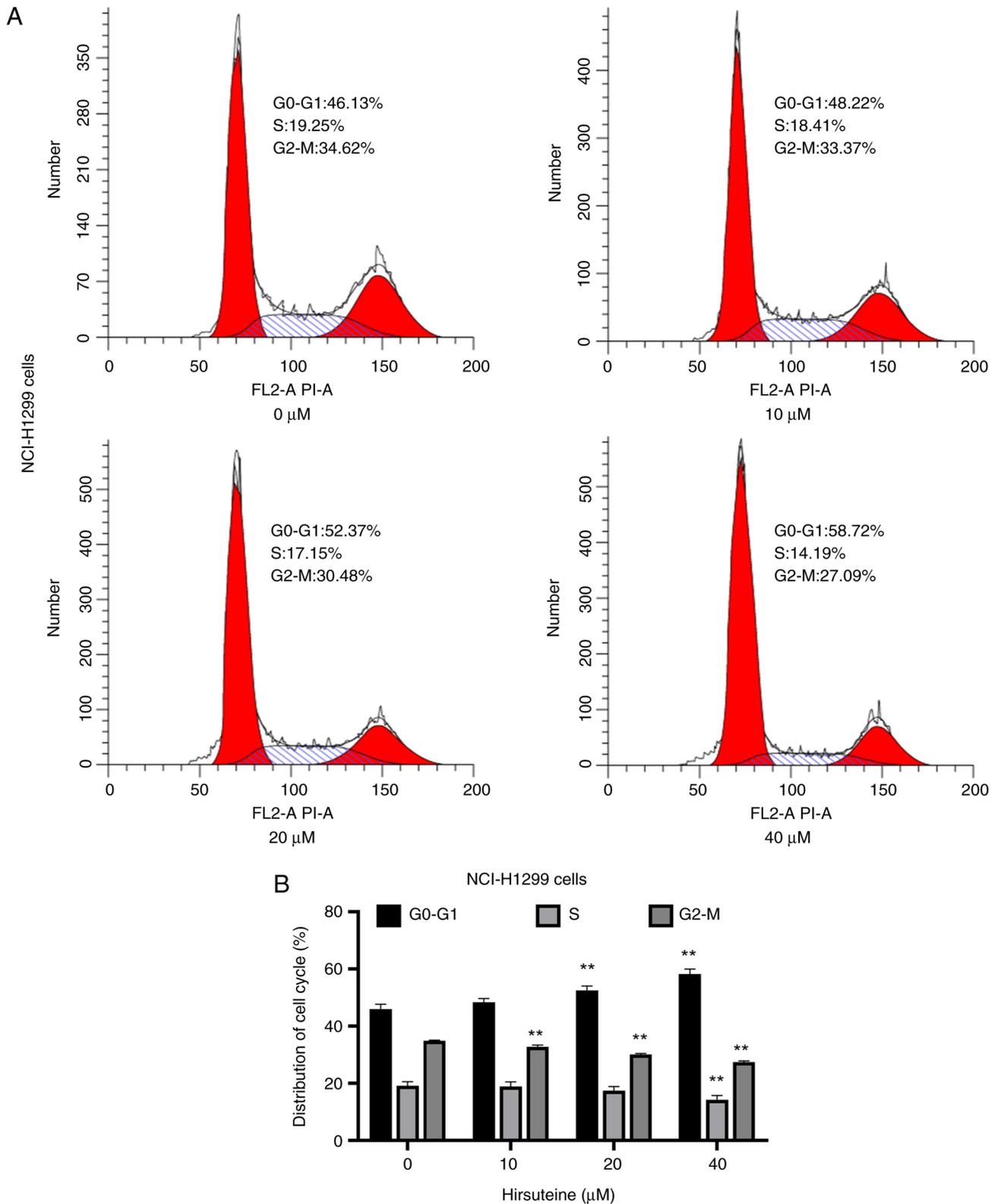
Figure 3. HTE causes NCI-H1299 cell cycle arrest. NCI-H1299 cells were treated with different doses of HTE for 48 h, and cell cycle analysis was performed by flow cytometry. (A) Cell cycle analysis of untreated and HTE-treated NCI-H1299 cells was performed by flow cytometry. (B) Statistical analysis of the cells in each cell cycle phase after treatment with HTE for 48 h. All data are expressed as the mean ± SD of three independent experiments. **P<0.01 compared with the control. HTE, hirsuteine.

Proteintech Group, Inc.), anti-Bcl-2 (cat. no. 12789-1-AP; Proteintech Group, Inc.), anti-Apaf1 (cat. no. A0751; ABclonal Biotech Co., Ltd.), anti-cytochrome C (cat. no. Ab133504; Abcam), anti-cleaved caspase-9 (cat. no. AF5240; Affinity

Biosciences), or anti-cleaved caspase-3 (cat. no. Ab32042; Abcam) antibodies, all diluted 1:1,000. The blots were then washed three times with TBST for 45 min, followed by incubation for 2 h with HRP-conjugated goat anti-rabbit IgG

(1:5,000; cat. no. BA1054) or goat anti-mouse IgG (1:5,000; cat. no. BA1051; both from Boster Biological Technology). Immunoblotted proteins were analyzed with the ChemiDoc XRS imaging system and QuantityOne software (Version 4.6.9; Bio-Rad Laboratories, Inc.).

Reverse transcription quantitative (RT-q) PCR analysis. Cells in the logarithmic phase were cultured in a six-well plate at a density of $1x10^6$ cells/well for 48 h. The cells were then treated with different doses of HTE for 48 h. Total RNA from the cultured cells was isolated using TRIzol® reagent (Invitrogen; Thermo Fisher Scientific, Inc.). Afterwards, cDNA synthesis was performed according to the protocol of the QuantiTect Reverse Transcription Kit (Invitrogen; Thermo Fisher Scientific, Inc.). qPCR was conducted on an ABI 7500 Fast Real-Time PCR system (Applied Biosystems; Thermo Fisher Scientific, Inc.) with TaqMan™ Multiplex Master Mix (Invitrogen; Thermo Fisher Scientific, Inc.) with the following thermocycling conditions: Denaturation at 95°C for 10 min and 40 cycles of 95°C for 30 sec, annealing for 30 sec at 60°C and extension for 20 sec at 72°C. The following primer sequences were used for the qPCR assay: Bax forward, 5'-AAGAAGCTG AGCGAGTGTCT-3' and reverse, 5'-GTTCTGATCAGTTCC GGCAC-3' (236 bp); Bcl-2 forward, 5'-GCCTTCTTTGAG TTCGGTGG-3' and reverse, 5'-GAAATCAAACAGAGG CCGCA-3' (192 bp); and GAPDH forward, 5'-TCAAGAAGG TGGTGAAGCAGG-3' and reverse, 5'-TCAAAGGTGGAG GAGTGGGT-3' (115 bp). All PCRs were performed in triplicate. Data were analyzed using the $2^{-\Delta\Delta Cq}$ method (33) with GAPDH as the reference gene for normalization.

Statistical analysis. The mean ± standard deviations of at least three independently conducted experiments were used to represent the data collected in all studies. All statistical analyses were performed using SPSS 23.0 software version (IBM Corp.). Significant differences were performed by one-way analysis of variance, followed by Bonferroni's test. A value of $P<0.05$ was considered to indicate a statistically significant difference.

Results

HTE suppresses NSCLC NCI-H1299 cell proliferation and colony formation. To investigate the effect of HTE on cell proliferation, the NCI-H1299 cell line was finally selected as the study cell line according to the pre-experimental data after the different concentrations of HTE were applied to different types of cancer cells (data not shown). According to the experimental results of CCK-8, it is assumed that the HTE solution is stable enough under the culture conditions. The cell proliferation inhibition rate of the HTE on NCI-H1299 cells at 72 h is more obvious than that at 48 h. Referring to previous literature, the treatment time point for follow-up analysis was set at 48 h (34). As revealed in Fig. 2A, the ability of HTE to inhibit the proliferation of NCI-H1299 cells significantly increased in a time- and concentration-dependent manner with half maximal inhibitory concentration values of 82.81, 43.74 and 27.02 μM at these three time points, respectively, when compared with the control group (Fig. 2A). Next, the impact of HTE on the proliferation of BEAS-2B and human hepatocyte
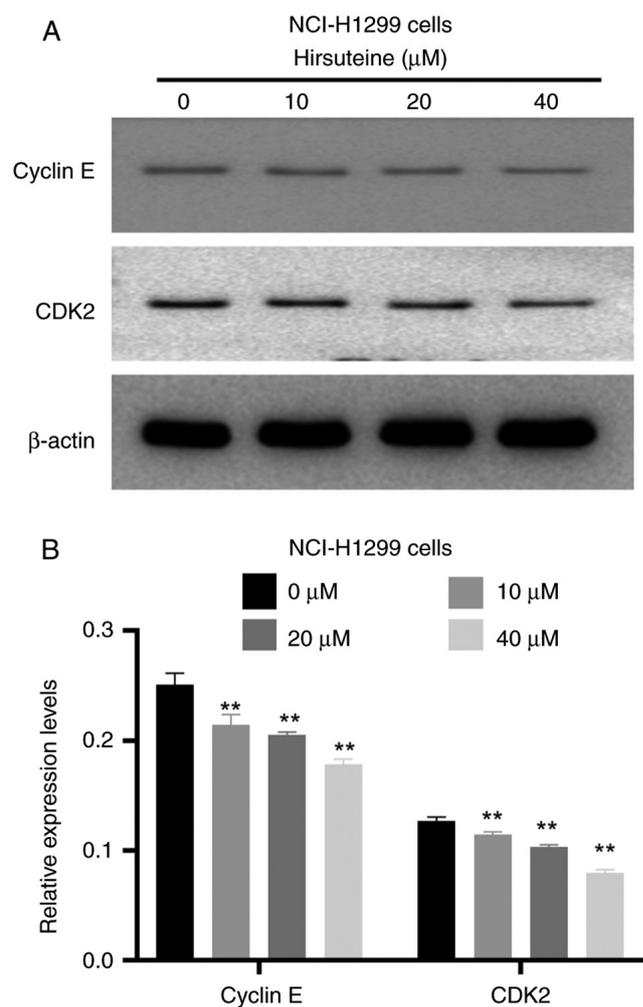
Figure 4. HTE regulates the activity of cyclin-CDK complexes and cell cycle progression. (A) The protein levels of cyclin E and CDK2 in NCI-H1299 cells treated with HTE as measured by western blotting. (B) Statistical analysis of cyclin E and CDK2 levels in NCI-H1299 cells. The protein level ratios were standardized according to the value of the control. All data are expressed as the mean ± SD of three independent experiments. **$P<0.01$ compared with the control. HTE, hirsuteine; CDK, cyclin-dependent kinase.

THLE-2 cells was explored using a CCK-8 assay. The results showed that the cell viability after HTE treatment in normal cells was >80% after 48 h of treatment at doses up to and including 80 μM; thus, HTE was considered to be non-toxic to these non-cancerous cell lines (Fig. 2B). To expand on these results, a colony formation assay was performed, which revealed that HTE treatment suppressed NCI-H1299 colony formation activity relative to control treatment (Fig. 2C and D). Based on the results, HTE inhibited NCI-H1299 cell proliferation and lowered NCI-H1299 colony formation activity whilst not exerting a notable effect on healthy human cells at the same doses.

HTE induces cell cycle arrest. Following treatment with several HTE doses for 48 h, the effect of HTE on NCI-H1299 cell cycle progression was investigated. In the diagram of the cell cycle, the red portion on the left represents G0-G1 phase, the curve marked in the middle represents S phase, and the red portion on the right indicates G2-M phase. Flow
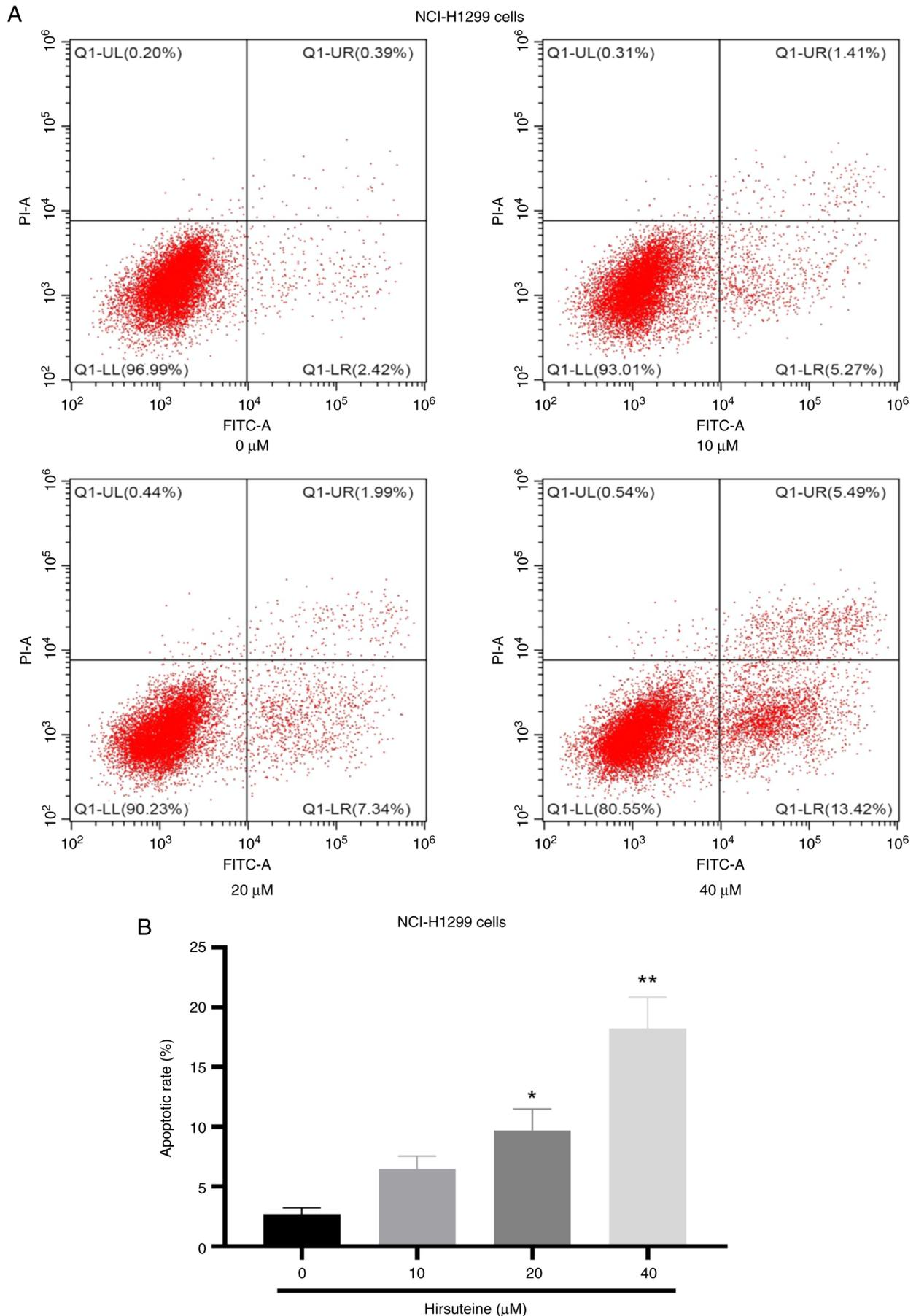
Figure 5. HTE induces NCI-H1299 cell apoptosis. (A) The apoptotic rate of NCI-H1299 cells treated with HTE was measured by Annexin V-FITC/PI double staining. (B) Statistical analysis of the apoptosis rates of NCI-H1299 cells treated with HTE. All data are expressed as the mean ± SD of three independent experiments. *P<0.05 and **P<0.01 compared with the control. HTE, hirsuteine.
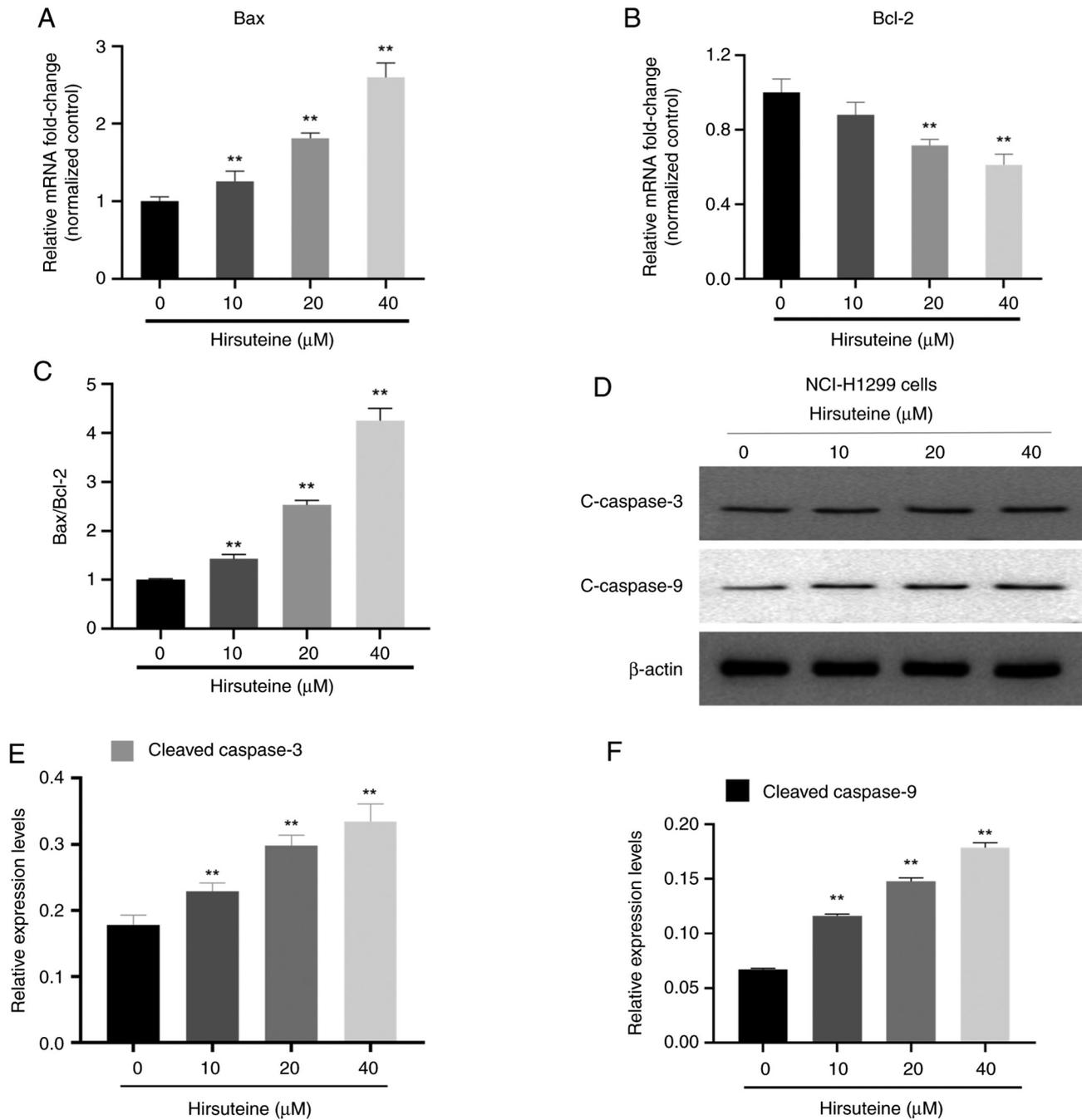
Figure 6. Effects of HTE on apoptosis-related mRNA and protein levels. After 48 h of treatment with different doses of HTE, the expression of Bax/Bcl-2 mRNA and cleaved caspase-3/9 protein in NCI-H1299 cells were measured by reverse transcription-quantitative PCR and western blotting. (A and B) Bar graphs of the mRNA levels of Bax and Bcl-2 in NCI-H1299 cells. (C) Bar graphs of the Bax/Bcl-2 ratio in NCI-H1299 cells. (D) The relative protein levels of cleaved caspase-3/9 in NCI-H1299 cells treated with HTE were measured by western blotting. (E and F) The ratios of protein levels were normalized to the value of the control group. All data are expressed as the mean ± SD of three independent experiments. **P<0.01 compared with the control. HTE, hirsuteine.

cytometric analysis revealed that HTE treatment (0, 10, 20 and 40 μM) was associated with an increase in the frequency of NCI-H1299 cells in G0/G1 phase. A significant increase in the proportion of NCI-H1299 cells in G0-G1 phase was observed in the HTE treatment groups (20 and 40 μM) (Fig. 3).

HTE decreases the levels of cyclin and CDK in NCI-H1299 cells. To investigate the mechanism by which the cell cycle is arrested in NCI-H1299 cells, the expression of cell cycle-related proteins was next determined via western blotting in HTE-treated cells.

Significant reductions in the CDK2 and cyclin-E expression levels were observed in NCI-H1299 cells treated with HTE (0, 10, 20 and 40 μM) (Fig. 4A and B), suggesting that HTE may be responsible for G0-G1 phase arrest.

HTE induces NCI-H1299 cell apoptotic death. As indicated in Fig. 5, the ability of HTE to induce NCI-H1299 cell apoptosis was next assessed via flow cytometry, which confirmed the increase in NCI-H1299 cell apoptosis frequency after treatment with HTE.
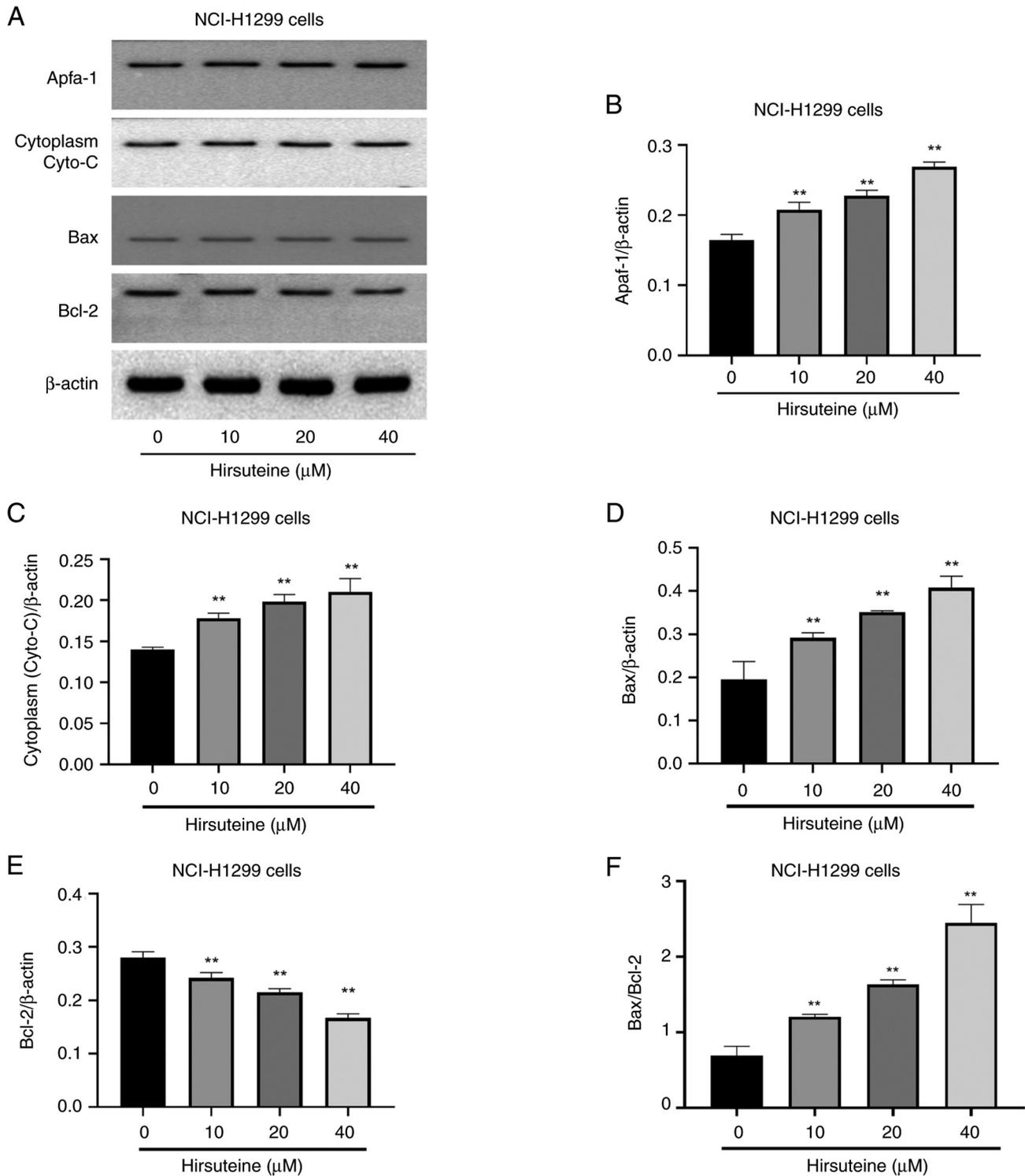
Figure 7. HTE induces NCI-H1299 cell apoptosis through the Bcl-2/Bax signaling pathway. (A) The protein levels of Apaf1, cytoplasmic Cyto-C, Bax, and Bcl-2 in NCI-H1299 cells treated with HTE were measured by western blotting. (B-E) Statistical analysis of the relative protein levels of Apaf1, cytoplasmic Cyto-C, Bax and Bcl-2 in NCI-H1299 cells treated with HTE. The ratios of protein levels were normalized to the value of the control. (F) Bar graphs of the ratios of Bax/Bcl-2 in NCI-H1299 cells. All data are expressed as the mean ± SD of three independent experiments. **P<0.01 compared with the corresponding control. HTE, hirsuteine; Cyto-C, cytochrome c.

HTE treatment alters the expression of apoptosis-related genes and proteins. To explore the mechanisms underlying HTE-induced apoptosis in these NSCLC cells, the cellular Bax and Bcl-2 levels were assessed following 48 h of treatment with this drug through RT-qPCR and western blot analyses. In the RT-qPCR experiments, the Bax mRNA levels increased in NCI-H1299 cells whereas the expression levels of Bcl-2 decreased following treatment with HTE. These effects were significant at HTE concentrations of 0, 10, 20 and 40 μM compared with untreated cells (P<0.05 or P<0.01) (Fig. 6A and B). HTE may decrease Bcl-2 mRNA levels while increasing the mRNA content of Bax, resulting in a higher

pro-apoptotic vs. anti-apoptotic protein ratio (Fig. 6C). The expression levels of cleaved caspase-3 and cleaved caspase-9 were analyzed using western blot ting to assess antiproliferative activity of HTE-induced NCI-H1299 cells, and the results indicated that the expression levels of cleaved caspase-3/9 increased following treatment with HTE (Fig. 6D-F). These results demonstrated that HTE could cause death in NCI-H1299 cells via a caspase-mediated mechanism.

HTE induces NCI-H1299 cell apoptotic death via the Bcl-2/Bax signaling pathway. Moreover, it was aimed to further understand the underlying mechanisms of HTE-induced apoptosis in NCI-H1299 cells. Western blotting was performed to determine the expression levels of the pro-apoptotic proteins and anti-apoptotic proteins Bax and Bcl-2, as well as cytoplasmic cytochrome c (Cyto-C) and Apaf1 *in vitro*. HTE treatment resulted in Bcl-2 downregulation and increased cytoplasmic Cyto-C, Bax and Apaf1 levels, causing the Bax/Bcl-2 ratio to be unbalanced (Fig. 7A-F), and the high-dose HTE group demonstrated a high level of expression in comparison with the control group ($P<0.05$ or $P<0.01$). By contrast, expression was lower in the low-dose HTE group than in the high-dose HTE group, indicating that HTE induces apoptosis in NCI-H1299 cells in a dose-dependent fashion. All of these data demonstrated that HTE activates the Bcl-2/Bax signaling pathway, causing apoptosis in NCI-H1299 cells.

Discussion

NSCLC is one of the principal causes of cancer-related morbidity and mortality (2). There has been increasing interest in finding natural compounds that can act as preventive and therapeutic agents for cancer treatment. UR is a well-known traditional Chinese herbal medicine that is used for the treatment of a variety of malignancies as well as other disorders, including hypertension and Parkinson's disease (34-37). HTE is a natural compound from the bark of UR, and few studies to date have explored the antiproliferative properties of this novel drug. In the present study, it was found that HTE treatment was sufficient to inhibit NCI-H1299 cells from proliferating as determined by CCK-8 and colony formation experiments, and subsequent Annexin V/PI staining demonstrated that this treatment may stimulate cell apoptosis and cell cycle arrest in these NSCLC cells. HTE was also able to modify the cell cycle by affecting apoptosis-related protein levels and upstream regulatory signaling pathways.

Cell cycle dysregulation is a hallmark of cancer. Under normal physiological conditions, the cell cycle exhibits tight multilayer regulation (38), carefully controlling the progression of the cell through G1 phase before entering into DNA synthesis, S phase, during which DNA is replicated, and the subsequent G2 phase. Cyclin-dependent kinases (CDKs) and their associated cyclins form complexes with one another to govern cell cycle regulation, and they are highly evolutionarily conserved in eukaryotic species (39-41), with substantial cyclin and CDK gene expansion and subfunctionalization observed across species (42-44). Adverse events related to ICIs are particularly challenging to control with adjuvant therapies because delayed (occasionally severe) toxicity may cause permanent injury to patients who may have had their

tumorigenic disease cured by surgery (13). The expression and activation of cell cycle mediators is deranged, particularly within the CDK-cyclin-RB pathways, and is involved in malignant transformation and tumor progression in lung cancer (45). In >90% of lung cancers, the cell cycle occurs as dysregulation, which causes the disorder of cell cycle mediators in expression and/or activation, particularly within the CDK-cyclin-RB pathways, and is closely related to malignant transformation and tumor progression, which destroys the cell proliferation mechanism controlling the growth of advanced NSCLC (45-47). However, the clinical trial results of evaluating single-dose CDK inhibitors in NSCLC and SCLC patients were disappointing. In addition, cell cycle regulation involves complex interactions of multiple signal pathways and mediators. Therefore, although targeted CDK family members may display preclinical activity in selective tumor models, they may not be sufficient to produce meaningful responses in more complex clinical environments (45). CDK inhibitors have favorable antitumor effects, but their lack of accuracy, side effects to biological targets and limitations of the therapeutic population lead to unsatisfactory therapeutic results. Therefore, embedding the CDK pathway in lung cancer treatment remains challenging (45). The current western blotting data indicated that HTE treatment reduces CDK2 and cyclin E levels in HTE-treated NCI-H1299 cells, causing cell cycle arrest in G0/G1 phase and an increase in the relative population of cells' G1 phase.

Apoptosis is an essential cellular process in which cells are constrained to self-destruction (48). Two classical activation pathways are involved in the initiation and regulation of apoptosis (49). The intrinsic apoptotic pathway is activated by stress-related intracellular signals, including the mitochondrial intermembrane protein Cyto-C, which initiates signal transduction cascades and eventually activates caspase-3. The intrinsic apoptotic pathway is regulated by a family of Bcl-2 proteins and has been broadly grouped into two key regulatory categories, including pro-apoptotic proteins (Bax, Bak and Bok/MTD) and anti-apoptotic proteins (including Bcl-2) (50). Numerous cancers exhibit overexpression of Bcl-2, which influences the onset, progression and chemoresistance of these tumors (51-53). Overexpression of Bax, by contrast, can induce apoptotic death (54). A reduction in mitochondrial membrane potential (MMP) occurs due to a drop in the relative anti-apoptotic to pro-apoptotic Bcl-2 family protein ratio and leads to apoptosis (55). HTE treatment in the present study resulted in significant downregulation of Bax expression, whereas Bax levels were significantly elevated upon treatment. The results showed that the ratio of Bax/Bcl-2 expression exhibited an increasing tendency with increasing HTE concentration, and this ratio increased significantly when the cells were stimulated by 10 and 25 μmol/l HTE. These findings complemented the prior findings of decreased cell viability and increased apoptosis, suggesting that HTE may impact NCI-H1299 cells by modulating the Bcl-2 family-dependent intrinsic apoptotic pathway. Notably, the expression levels of the Bcl-2 family members, and particularly the ratio of pro-apoptotic Bax/anti-apoptotic Bcl-2, are widely used to indicate an intrinsic apoptotic mechanism (56).

The initiation of apoptotic signaling cascades within cells can drive increased mitochondrial permeability (57). Bax is

widely distributed on the outer mitochondrial membrane to control MMP and thereby influences the release of Cyto-C and other drivers of apoptotic death (58). The released activated cytochrome can, in turn, bind to Apaf1 and thereby activate caspase-9 (59,60), subsequently stimulating caspase-3 and caspase-7 to initiate apoptotic cascade signaling pathways (57). The expression of these apoptosis-related proteins was investigated in NCI-H1299 cells, and HTE administration was identified to cause dose-dependent apoptosis in these NSCLC cells. HTE was also linked to increases in Apaf1, Bax, cytoplasmic Cyto-C, cleaved-caspase-3 and -9 levels, as well as the downregulation of Bcl-2 expression. These data suggested that HTE can thus initiate the mitochondrial-mediated signaling pathway of apoptosis in NCI-H1299 cells by modulating the relative Bcl-2-related protein levels.

Caspases are important in the pro-apoptotic process. Caspase-8 is involved in extrinsic (mitochondrial) apoptosis pathways, whereas caspase-9 is involved in intrinsic (mitochondrial) apoptosis pathways (61). The increase in the ratio of Bax/Bcl-2 promotes mitochondrial dysfunction, the release of some apoptotic factors, and caspase-9 activation. Then, active caspase-9 cleaves the downstream apoptosis effector caspase-3 (62). When Cyto-C is transferred to the cytoplasm from the mitochondria, it forms a large multiprotein complex with Apaf1, procaspase-9 and Cyto-C, and activation of the intrinsic mitochondria-mediated pathway occurs. In the current investigation, HTE significantly increased the activity of Bax, caspase-3, and caspase-9 in NCI-H1299 cells. This indicated that the mitochondria-mediated apoptosis pathway was activated, and that subsequent apoptosis was induced by the caspase-dependent and Cyto-C-mediated pathways. In addition, HTE-induced apoptosis is also involved the delivery of the flavoprotein apoptosis-inducing factor (AIF) from the mitochondria to the cytoplasm through a subsequent dose-dependent shift in the nucleus. The expulsion of AIF from mitochondria to the nucleus, while translocating from the cytosol, interacts with DNA, thus functioning through a caspase-independent pathway. Similar findings have been previously reported, stating that mitochondria-mediated pathways are important in *A. adenophora*-induced apoptosis and cell death (63-65). HTE may also cause cell death and apoptosis as a result of mitochondria-mediated pathway stimulation.

The present study demonstrated that HTE could inhibit NCI-H1299 cell proliferation by inducing apoptosis through the Bax/Bcl-2 signaling pathway and induce G0/G1 phase arrest through cyclin E- and CDK2-mediated mechanisms. The current findings offer a theoretical basis to understand the underlying mechanism of the antiproliferative effect of HTE and show that this compound can be used as an effective natural medicine in the treatment and prevention of human NSCLC.

Ultrahigh-Performance Liquid Chromatography-Mass Spectrometry (UPLC-MS) was used for the detection of HTI and HTE in tissues to help understand in an improved way the pharmacological mechanisms of HTI and HTE (28,66). However, certain limitations to the present study should be noted. Numerous compounds were screened with different types of cells in the pre-experiment including HTI and HTE. According to the results of the preliminary experiment CCK-8,

the anti-proliferation effect of HTI on cells is stronger than that of HTE. As HTI has been previously investigated before, the activity of HTE was researched (34). The difference between the anti-proliferative effect of HTI and HTE appears in the pre-experimental data (data not shown), as a reference for the preliminary research of this project. In the future study by the authors, the data of the pre-experiment shall be included in the manuscript. Furthermore, the antitumor effects of HTE were not examined in a lung-xenografted model in nude mice. Moreover, another weakness was that only one cell line was used in the present study. The NCI-H1299 cell line was finally selected as the study cell line according to the pre-experimental data (data not shown) after the different concentrations of HTE were applied to different types of cancer cells. Using additional cell lines such as A549 is recommended in future studies. The stability of the HTE is only based on the results of CCK-8, and no specific test has been carried out on the stability. In addition, UPLC-MS technology will be used to detect the concentration of HTE in patient lung tissues and *in vivo* experiments will be increased in future research by the authors. In conclusion, the results of the present study revealed that HTE inhibits cell proliferation in NCI-H1299 cells and induces apoptosis via a mitochondrial-mediated signaling pathway. The current study provides evidence for the development of HTE as an anti-lung drug.

In summary, the present data revealed that HTE can suppress NCI-H1299 cell proliferation by regulating the proteins CDK2 and cyclin E, inducing their apoptotic death via the mitochondrial signaling pathway. The present study not only highlights a promising new treatment for human NSCLC but also offers a sound theoretical foundation for the proliferative activity of this deadly disease.

Availability of data and materials

The datasets used and/or analyzed during the current study are available from the corresponding author on reasonable request.

Authors' contributions

XY and BY made substantial contributions to conception and design of the research. XY analyzed the data, performed the experiments, prepared the figures and reviewed or authored drafts of the manuscript. HQ, YL and BD collected cell samples for qPCR and made substantial contributions to acquisition of data, or analysis and interpretation of data. YP made substantial contributions to analysis and interpretation of data. BY made substantial contributions to the revision of the manuscript and gave final approval of the manuscript to be published. XY and BY confirm the authenticity of all the raw data. All authors read and approved the final version of the manuscript.

Ethics approval and consent to participate

Not applicable.

Patient consent for publication

Not applicable.

Competing interests

The authors declare that they have no competing interests.

References

1. Torre LA, Siegel RL and Jemal A: Lung cancer statistics. Adv Exp Med Biol 893: 1-19, 2016.
2. Duma N, Santana-Davila R and Molina JR: Non-small cell lung cancer: Epidemiology, screening, diagnosis, and treatment. Mayo Clin Proc 94: 1623-1640, 2019.
3. Brueckl WM, Achenbach HJ, Ficker JH and Schuette W: Erlotinib treatment after platinum-based therapy in elderly patients with non-small-cell lung cancer in routine clinical practice-results from the ElderTac study. BMC Cancer 18: 333, 2018.
4. Hirsch FR, Sequist LV, Gore I, Mooradian M, Simon G, Croft EF, DeVincenzo D, Munley J, Stein D, Freivogel K, et al: Long-term safety and survival with gefitinib in select patients with advanced non-small cell lung cancer: Results from the US IRESSA clinical access program (ICAP). Cancer 124: 2407-2414, 2018.
5. Ciuleanu T, Stelmakh L, Cicenas S, Miliauskas S, Grigorescu AC, Hillenbach C, Johannsdottir HK, Klughammer B and Gonzalez EE: Efficacy and safety of erlotinib versus chemotherapy in second-line treatment of patients with advanced, non-small-cell lung cancer with poor prognosis (TITAN): A randomised multicentre, open-label, phase 3 study. Lancet Oncol 13: 300-308, 2012.
6. Olszewski AJ, Ali S and Witherby SM: Disparate survival trends in histologic subtypes of metastatic non-small cell lung cancer: A population-based analysis. Am J Cancer Res 5: 2229-2240, 2015.
7. Chang JS, Chen LT, Shan YS, Lin SF, Hsiao SY, Tsai CR, Yu SJ and Tsai HJ: Comprehensive analysis of the incidence and survival patterns of lung cancer by histologies, including rare subtypes, in the era of molecular medicine and targeted therapy: A nation-wide cancer registry-based study from Taiwan. Medicine (Baltimore) 94: e969, 2015.
8. Jonna S and Subramaniam DS: Molecular diagnostics and targeted therapies in non-small cell lung cancer (NSCLC): An update. Discov Med 27: 167-170, 2019.
9. Herbst RS, Morgensztern D and Boshoff C: The biology and management of non-small cell lung cancer. Nature 553: 446-454, 2018.
10. Wolchok JD: PD-1 blockers. Cell 162: 937, 2015.
11. Johnson DB, Sullivan RJ and Menzies AM: Immune checkpoint inhibitors in challenging populations. Cancer 123: 1904-1911, 2017.
12. Ma K, Jin Q, Wang M, Li X and Zhang Y: Research progress and clinical application of predictive biomarker for immune checkpoint inhibitors. Expert Rev Mol Diagn 19: 517-529, 2019.
13. de Miguel M and Calvo E: Clinical challenges of immune checkpoint inhibitors. Cancer Cell 38: 326-333, 2020.
14. Bando Y, Furukawa J, Terakawa T, Harada K, Hinata N, Nakano Y and Fujisawa M: Treatment outcomes of molecular targeted therapy following nivolumab in metastatic renal cell carcinoma. Jpn J Clin Oncol 51: 1313-1318, 2021.
15. Zhang J, Xu D, Zhou Y, Zhu Z and Yang X: Mechanisms and implications of CDK4/6 inhibitors for the treatment of NSCLC. Front Oncol 11: 676041, 2021.
16. Koehn FE and Carter GT: The evolving role of natural products in drug discovery. Nat Rev Drug Discov 4: 206-220, 2005.
17. Horie S, Yano S, Aimi N, Sakai S and Watanabe K: Effects of hirsutine, an antihypertensive indole alkaloid from Uncaria rhynchophylla, on intracellular calcium in rat thoracic aorta. Life Sci 50: 491-498, 1992.
18. Ndagijimana A, Wang X, Pan G, Zhang F, Feng H and Olaleye O: A review on indole alkaloids isolated from Uncaria rhynchophylla and their pharmacological studies. Fitoterapia 86: 35-47, 2013.
19. Nakazawa T, Banba K, Hata K, Nihei Y, Hoshikawa A and Ohsawa K: Metabolites of hirsuteine and hirsutine, the major indole alkaloids of Uncaria rhynchophylla, in rats. Biol Pharm Bull 29: 1671-1677, 2006.
20. Xian YF, Lin ZX, Mao QQ, Hu Z, Zhao M, Che CT and Ip SP: Bioassay-guided isolation of neuroprotective compounds from Uncaria rhynchophylla against beta-amyloid-induced neurotoxicity. Evid Based Complement Alternat Med 2012: 802625, 2012.
21. Lan YL, Zhou JJ, Liu J, Huo XK, Wang YL, Liang JH, Zhao JC, Sun CP, Yu ZL, Fang LL, et al: Uncaria rhynchophylla ameliorates Parkinson's disease by inhibiting HSP90 expression: Insights from quantitative proteomics. Cell Physiol Biochem 47: 1453-1464, 2018.
22. Liu CH, Lin YW, Tang NY, Liu HJ and Hsieh CL: Neuroprotective effect of Uncaria rhynchophylla in kainic acid-induced epileptic seizures by modulating hippocampal mossy fiber sprouting, neuron survival, astrocyte proliferation, and S100B expression. Evid Based Complement Alternat Med 2012: 194790, 2012.
23. Ozaki Y: Pharmacological studies of indole alkaloids obtained from domestic plants, Uncaria rhynchophylla Miq. and Amsonia elliptica Roem. et Schult. Nihon Yakurigaku Zasshi 94: 17-26, 1989 (In Japanese).
24. Ozaki Y: Vasodilative effects of indole alkaloids obtained from domestic plants, Uncaria rhynchophylla Miq. and Amsonia elliptica Roem. et Schult. Nihon Yakurigaku Zasshi 95: 47-54, 1990 (In Japanese).
25. Yuzurihara M, Ikarashi Y, Goto K, Sakakibara I, Hayakawa T and Sasaki H: Geissoschizine methyl ether, an indole alkaloid extracted from Uncariae Ramulus et Uncus, is a potent vasorelaxant of isolated rat aorta. Eur J Pharmacol 444: 183-189, 2002.
26. Nakamura Y, Ishida Y, Kondo M and Shimada S: Yokukansan contains compounds that antagonize the 5-HT$_3$ receptor. Phytomedicine 43: 120-125, 2018.
27. Mimaki Y, Toshimizu N, Yamada K and Sashida Y: Anti-convulsion effects of choto-san and chotoko (Uncariae Uncis cam Ramlus) in mice, and identification of the active principles. Yakugaku Zasshi 117: 1011-1021, 1997 (In Japanese).
28. Wang M, Guo J, Wang Z, Zhang G, Yu H, Chang R and Chen A: Simultaneous separation and determination of hirsutine and hirsuteine by cyclodextrin-modified micellar electrokinetic capillary chromatography. Phytochem Anal 31: 112-118, 2020.
29. Huang BY, Zeng Y, Li YJ, Huang XJ, Hu N, Yao N, Chen MF, Yang ZG, Chen ZS, Zhang DM and Zeng CQ: Uncaria alkaloids reverse ABCB1-mediated cancer multidrug resistance. Int J Oncol 51: 257-268, 2017.
30. Shimada Y, Goto H, Itoh T, Sakakibara I, Kubo M, Sasaki H and Terasawa SK: Evaluation of the protective effects of alkaloids isolated from the hooks and stems of Uncaria sinensis on glutamate-induced neuronal death in cultured cerebellar granule cells from rats. J Pharm Pharmacol 51: 715-722, 1999.
31. Kawakami Z, Kanno H, Ikarashi Y and Kase Y: Yokukansan, a kampo medicine, protects against glutamate cytotoxicity due to oxidative stress in PC12 cells. J Ethnopharmacol 134: 74-81, 2011.
32. Meng J, Su R, Wang L, Yuan B and Li L: Inhibitory effect and mechanism of action (MOA) of hirsutine on the proliferation of T-cell leukemia Jurkat clone E6-1 cells. PeerJ 9: e10692, 2021.
33. Livak KJ and Schmittgen TD: Analysis of relative gene expression data using real-time quantitative PCR and the 2(-Delta Delta C(T)) method. Methods 25: 402-408, 2001.
34. Zhang R, Li G, Zhang Q, Tang Q, Huang J, Hu C, Liu Y, Wang Q, Liu W, Gao N and Zhou S: Hirsutine induces mPTP-dependent apoptosis through ROCK1/PTEN/PI3K/GSK3β pathway in human lung cancer cells. Cell Death Dis 9: 598, 2018.
35. Chen XX, Leung GP, Zhang ZJ, Xiao JB, Lao LX, Feng F, Mak JC, Wang Y, Sze SC and Zhang KY: Proanthocyanidins from Uncaria rhynchophylla induced apoptosis in MDA-MB-231 breast cancer cells while enhancing cytotoxic effects of 5-fluorouracil. Food Chem Toxicol 107: 248-260, 2017.
36. Lee JS, Kim J, Kim BY, Lee HS, Ahn JS and Chang YS: Inhibition of phospholipase cgamma1 and cancer cell proliferation by triterpene esters from Uncaria rhynchophylla. J Nat Prod 63: 753-756, 2000.
37. Shim JS, Kim HG, Ju MS, Choi JG, Jeong SY and Oh MS: Effects of the hook of Uncaria rhynchophylla on neurotoxicity in the 6-hydroxydopamine model of Parkinson's disease. J Ethnopharmacol 126: 361-365, 2009.
38. Wang Y, Ji P, Liu J, Broaddus RR, Xue F and Zhang W: Centrosome-associated regulators of the G(2)/M checkpoint as targets for cancer therapy. Mol Cancer 8: 8, 2009.

39. Endicott JA and Noble ME: Structural principles in cell-cycle control: Beyond the CDKs. Structure 6: 535-541, 1998.
40. Coudreuse D and Nurse P: Driving the cell cycle with a minimal CDK control network. Nature 468: 1074-1079, 2010.
41. Harashima H, Dissmeyer N and Schnittger A: Cell cycle control across the eukaryotic kingdom. Trends Cell Biol 23: 345-356, 2013.
42. Cao L, Chen F, Yang X, Xu W, Xie J and Yu L: Phylogenetic analysis of CDK and cyclin proteins in premetazoan lineages. BMC Evol Biol 14: 10, 2014.
43. Li Z: Regulation of the cell division cycle in trypanosoma brucei. Eukaryot Cell 11: 1180-1190, 2012.
44. Gutierrez C: The arabidopsis cell division cycle. Arabidopsis Book 7: e0120, 2009.
45. Qin A, Reddy HG, Weinberg FD and Kalemkerian GP: Cyclin-dependent kinase inhibitors for the treatment of lung cancer. Expert Opin Pharmacother 21: 941-952, 2020.
46. Otto T and Sicinski P: Cell cycle proteins as promising targets in cancer therapy. Nat Rev Cancer 17: 93-115, 2017.
47. No authors listed: Milestones in cell division. Nat Cell Biol 3: E265, 2001.
48. Fulda S, Gorman AM, Hori O and Samali A: Cellular stress responses: Cell survival and cell death. Int J Cell Biol 2010: 214074, 2010.
49. Long S, Wilson M, Bengtén E, Clem LW, Miller NW and Chinchar VG: Identification and characterization of a FasL-like protein and cDNAs encoding the channel catfish death-inducing signaling complex. Immunogenetics 56: 518-530, 2004.
50. Youle RJ and Strasser A: The BCL-2 protein family: Opposing activities that mediate cell death. Nat Rev Mol Cell Biol 9: 47-59, 2008.
51. Haldar S, Negrini M, Monne M, Sabbioni S and Croce CM: Down-regulation of bcl-2 by p53 in breast cancer cells. Cancer Res 54: 2095-2097, 1994.
52. Hwang KT, Han W, Kim J, Moon HG, Oh S, Song YS, Kim YA, Chang MS and Noh DY: Prognostic influence of BCL2 on molecular subtypes of breast cancer. J Breast Cancer 20: 54-64, 2017.
53. Jamous A and Salah Z: WW-domain containing protein roles in breast tumorigenesis. Front Oncol 8: 580, 2018.
54. Jensen K, WuWong DJ, Wong S, Matsuyama M and Matsuyama S: Pharmacological inhibition of Bax-induced cell death: Bax-inhibiting peptides and small compounds inhibiting Bax. Exp Biol Med (Maywood) 244: 621-329, 2019.
55. Nemec KN and Khaled AR: Therapeutic modulation of apoptosis: Targeting the BCL-2 family at the interface of the mitochondrial membrane. Yonsei Med J 49: 689-697, 2008.
56. Chresta CM, Masters JR and Hickman JA: Hypersensitivity of human testicular tumors to etoposide-induced apoptosis is associated with functional p53 and a high Bax:Bcl-2 ratio. Cancer Res 56: 1834-1841, 1996.
57. Strasser A, Cory S and Adams JM: Deciphering the rules of programmed cell death to improve therapy of cancer and other diseases. EMBO J 30: 3667-3683, 2011.
58. Jiang X and Wang X: Cytochrome C-mediated apoptosis. Annu Rev Biochem 73: 87-106, 2004.
59. Eskes R, Antonsson B, Osen-Sand A, Montessuit S, Richter C, Sadoul R, Mazzei G, Nichols A and Martinou JC: Bax-induced cytochrome C release from mitochondria is independent of the permeability transition pore but highly dependent on Mg2+ ions. J Cell Biol 143: 217-224, 1998.
60. Lee CH, Shih YL, Lee MH, Au MK, Chen YL, Lu HF and Chung JG: Bufalin induces apoptosis of human osteosarcoma U-2 OS cells through endoplasmic reticulum stress, caspase- and mitochondria-dependent signaling pathways. Molecules 22: 437, 2017.
61. Monie TP and Bryant CE: Caspase-8 functions as a key mediator of inflammation and pro-IL-1β processing via both canonical and non-canonical pathways. Immunol Rev 265: 181-193, 2015.
62. Vaculova A and Zhivotovsky B: Caspases: Determination of their activities in apoptotic cells. Methods Enzymol 442: 157-181, 2008.
63. He Y, Chen W, Hu Y, Luo B, Wu L, Qiao Y, Mo Q, Xu R, Zhou Y, Ren Z, *et al*: E. adenophorum induces cell cycle and apoptosis of renal cells through mitochondrial pathway and caspase activation in saanen goat. PLoS One 10: e0138504, 2015.
64. He Y, Mo Q, Hu Y, Chen W, Luo B, Wu L, Qiao Y, Xu R, Zhou Y, Zuo Z, *et al*: E. adenophorum induces cell cycle arrest and apoptosis of splenocytes through the mitochondrial pathway and caspase activation in saanen goats. Sci Rep 5: 15967, 2015.
65. He Y, Mo Q, Luo B, Qiao Y, Xu R, Zuo Z, Deng J, Nong X, Peng G, He W, *et al*: Induction of apoptosis and autophagy via mitochondria- and PI3K/Akt/mTOR-mediated pathways by E. adenophorum in hepatocytes of saanen goat. Oncotarget 7: 54537-54548, 2016.
66. Zhou Q, Ma J and Chen L: Tissue distribution of hirsutine and hirsuteine in mice by ultrahigh-performance liquid chromatography-mass spectrometry. J Anal Methods Chem 2020: 7204315, 2020.